ELECTRONIC SUPPORTING INFORMATION

Light-Induced Switching of Polymer-Surfactant Interactions Enables Controlled Polymer Thermoresponsive Behaviour

Eric Weißenborn,[a] Jörn Droste,[b] Michael Hardt, [a] Daniel Schlattmann,[a] Celine Tennagen, [b] Christian Honnigfort, [a] Monika Schönhoff, [a] Michael Ryan Hansen [b] and Björn Braunschweig [a]

[a.] Institute of Physical Chemistry and Center for Soft Nanoscience (SoN) Westfälische Wilhelms Universität Münster Corrensstraße 28-30, 48149 Münster, Germany

[b.] Institute of Physical Chemistry, Westfälische Wilhelms Universität Münster, Corrensstraße 28-30, 48149 Münster, Germany

* braunschweig@uni-muenster.de

1 Experimental Procedures

1.1 Sample Preparation.

The required glassware was precleaned with an Alconox solution (Sigma-Aldrich, now Merck) and rinsed several times with ultrapure water (18.2 MΩ cm, total organic carbon <3 ppm) which was obtained from Millipore Reference A+ purification system. The dried glassware was immersed in a bath with concentrated sulfuric acid (98 %, Carl Roth) and Nochromix (Godax Labs, USA) for at least 12 hours. Afterwards the glassware was rinsed several times with ultrapure water to remove remaining acid and dried with nitrogen gas (99.999 %, Westfalen, Germany).

The thermoresponsive polymer hydroxypropyl cellulose (HPC) (≥95 %, 1 MDa, Sigma-Aldrich) was used as received. For the stock solutions the necessary amount of HPC was dissolved in ultrapure water and stirred for several days until complete dissolution was reached. The *n*-butyl-arylazopyrazole butyl sulfonate (butyl-AAPC_4S, here in short AAP) was synthesized by as described previously.[1] For the irradiation of the samples two LEDs with emission wavelengths of 365 nm (UV) and 520 nm (green) were used. The experiments have been done under light exclusion and within 5 hours to minimize errors due to thermal relaxation.

1.2 Dynamic Light Scattering (DLS).

In this work the Zetasizer Nano ZSP from Malvern Panalytical has been used which consists of a He-Ne Laser (10 mW, 633nm) and a detector that recorded the backscattered light at an angle of 173°. To avoid multiple-scattering effects due to the turbidity above the LCST, a lower HPC concentration of 0.05 g/L was used for the DLS experiments and the solutions were filtered with a 0.2 µm syringe filter before each measurement. The temperature of the solutions was adjusted by a Peltier-element in the measurement chamber of the Zetasizer ZSP. For the determination of the lower critical solution temperature (LCST) the intensity of the backscattering light of unfiltered mixtures of 0.5 g/L HPC and AAP were measured with the same setup as mentioned above.

1.3 UV/Vis Spectroscopy.

The UV/Vis spectra (Figure S1a) were recorded with double-beam spectrometer (Perkin Elmer, Lambda 650). For the measurement at 50 °C a thermostat (Witeg Germany, WCR-8) was attached to a homebuild cuvette holder. The temperature in the cuvette was calibrated with a PT100 temperature sensor. The turbidity measurements were performed with a double beam spectrometer (JASCO Germany GmbH, V-770) with a peltier-thermo element (PAC743R) for the temperature control. For that, the samples' transmission at a wavelength of 700 nm was monitored as lower wavelengths can affect/switch the AAP surfactants.

1.4 Shear Rheology.

The rheology experiments were done with the shear rheometer MCR 102 (Anton Paar, Austria) using a cone-plate geometry with a cone radius of 2.5 cm and a cone angle of 2°. The samples were continuously irradiated in a modified setup where the metal plate under the probe has been exchanged with a glass plate to incorporate irradiation with green and UV using the same LEDs as noted above. The temperature was adjusted with a Peltier element below the glass plate. The evaporation of the solution was minimized by placing the cone-plate geometry under a closed hood.

1.5 Nuclear Magnetic Resonance (NMR).

All ^{1}H HR-MAS experiments were conducted on a Bruker AVANCE NEO spectrometer (11.76 T, $\nu_L(^1H)$ = 500.39 MHz) using a Bruker 4.0 mm H/F/X MAS DVT probe with magic-angle gradient coils and 4.0 mm o.d. ZrO_2 HR-MAS rotors with Kel-F© caps. An upper Teflon spacer was placed on top of the sample and sealed with a Kel-F© screw. Adamantane was used to determine the radio-frequency (rf) pulse length ($t_{\pi/2}$ = 4.0 µs). All 1D and 2D NMR experiments were recorded employing a MAS frequency of 5.0 kHz. For the 2D ^{1}H-^{1}H experiments spectrum the HDO signal was used for the ^{2}H lock. A total of 256 rotor-synchronized t_1 increments were recorded for the *radio-frequency dipolar-driven recoupling* (RFDR, xy-8 phase cycling)[5,6] experiments. 64 rotor periods of dipolar recoupling (102.4 ms) were used. The recycle delay was set to 2.0 s. The variable-temperature ^{1}H HR-MAS spectra were locked to the HDO signal and afterwards referenced to the temperature-dependent chemical shift of the HDO signal.[7] All ^{1}H MAS NMR spectra were recorded with a recycle delay of 10.0 s to obtain quantitative signal intensities. At each new temperature, the sample was equilibrated for 10 min before the measurements were started. The temperature was calibrated using ethylene glycol as an external reference.[8] A 2 Hz exponential linebroadening was applied to all FIDs before Fourier transformation. Data processing and analysis were done using the Bruker Topspin4.0.9 Software and Python. Light irradiation of the sample was performed ex situ directly before the experiments. The samples were irradiated for one hour with green (520 nm) and UV (365 nm) light, respectively.

1.6 Differential Scanning Calorimetry (DSC)

Experiments were performed on a micro DSC (micro DSC III, Setaram, France). Acquisition and evaluation of raw data were done using the software package *Calisto Data Acquisition* (v2.08) and *Data Processing* (v2.08) (*AKTS, Siders, Switzerland)*. The DSC setup consisted of two cells, one filled with the sample, the other filled with the same volume of water. Volumes were always 320 µL, samples were exposed to UV or green light for at least 30 min each. Prior to the measurement, the sample was exposed to a temperature cycle from 35 to 45 °C and back at a rate of 1.5 °C/min to avoid artefacts arising from air bubbles in the sample container. The temperature was then increased from 35 to 60 °C at a heating rate of 0.4 °C/min for the phase transition measurement. From the heat flow traces the onset temperatures T_{DSC} of the endothermic phase transition peaks were extracted.

2 Supplementary Results

The addition of APP surfactants to the HPC solution under green light leads to changes in the polymers phase transition as discussed in detail in the main text. The following Table S1 summarizes the results for the determined LCST's under different irradiation conditions for all the complementary experiments that we have performed in this study (DLS, NMR, rheology, turbidity). As the different techniques require different concentrations to observe the apparent changes without strong artifacts (e.g. multiple scattering for DLS), two HPC concentrations had been used: a high concentration (10 g/L) for the NMR and shear rheology experiments and a low concentration (0.5 g/L) for DLS, transmission and DSC experiments.

Table S1. Lower critical solution temperature (LCST) determined by different measurement techniques and for different AAP concentrations. The green and purple color indicate irradiation with green (520 nm) and UV light (365 nm). Abbreviations: NMR = ^{1}H HR-MAS NMR experiments; Visc. = viscosity experiments; DLS = Dynamic Light Scattering; Trans, = transmission experiments at 700 nm; DSC = Differential Scanning Calorimetry.

c_{AAP} / mM	*T* / °C (NMR,1)[a]	*T* / °C (NMR,2)[a]	*T* / °C (Visc)	*T* / °C (DLS)	*T* / °C (Trans)	*T* / °C (DSC)	*T* / °C (NMR,1)[a]	*T* / °C (NMR,2)[a]	*T* / °C (Visc)	*T* / °C (DLS)	*T* / °C (Trans)	*T* / °C (DSC)
	10 g/L HPC			0.5 g/L HPC			10 g/L HPC			0.5 g/L HPC		
0	44.0	43.3	43.6	42.3	43.8	42.8	44.0	43.3	43.6	42.3	43.8	42.8
0.1	-	-	-	42.1	42.8	42.4	-	-	-	42.1	43.6	43.0
0.2	-	-	-	40.3	42.2	40.9	-	-	-	42,0	43.6	42.8
0.4	-	-	-	42.2	40.8	45.2	-	-	-	42.1	43.6	42.8
0.7	-	-	-	46.8	48.6	46.8	-	-	-	42.1	43.6	42.8
1	42.4	42.5	39.1	>50	>50	-[c]	-[c]	-[c]	43.6	42.2	43.6	-[c]
2.5	42.8	44.6	50	-	-	-	43.0	42.6	43.5	-	-	-
5	52.4[b]	88.6[b]	>60	-	-	-	40.3	41.7	41.8	-	-	-
10	72.1[b]	137.9[b]	-[c]	-	-	-	40.1	40.6	-[c]	-	-	-

[a] NMR,1: δ(^{1}H) = 1.1 ppm (side-chain); NMR,2: δ(^{1}H) = 3.0 - 4.0ppm (backbone)

[b] No plateau was reached at higher temperatures (< 82 °C).

[c] This concentration was not measured.

2.1 UV/Vis Spectroscopy.

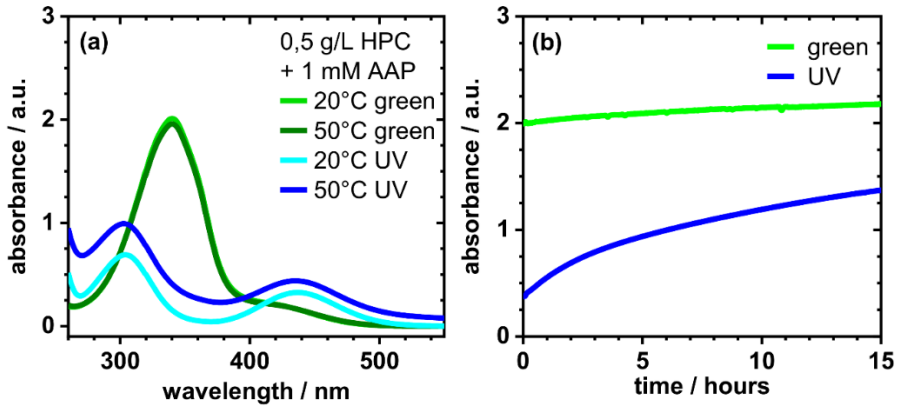

Figure S1. (a) UV/Vis absorbance spectra for different irradiation of the samples and at different temperatures. Concentration were 0.5 g/L HPC and 1 mM AAP. (b) Kinetic changes in optical absorbance at 342 nm of a mixture consisting of 0.5 g/L HPC and 1 mM AAP at 50 °C under green (green line) or UV (blue line) irradiation using a cuvette with an optical path length of 1 mm.

The absorption spectra of a HPC/AAP mixture at 20 °C as well as at 50 °C are shown in Figure S1a. The maximum absorbance at 20 °C at 340 nm (*E*) and 304 nm (*Z*) is consistent with previous reports by Honnigfort et al.[1] At temperatures above the LCST (50 °C) the spectra of the *E*-isomer remains unaffected whereas the spectra of the *Z*-isomer shows an increased absorbance at low wavelengths due to an increased turbidity of the sample. The absence of the turbidity under green light is a first indication of the possible light induced LCST displacement. The stability of the *Z*-isomer at 50 °C is evaluated by observing the absorbance at 342 nm where the maximal difference of the two absorption spectra of the isomers is located (Figure S1b) The slightly increase of the absorbance under green light occurs despite of the sealing of the sample due to the evaporation of the solvent. Assuming nearly complete transfer from the *E*- to the *Z*- isomer by UV light, after 5 h still two thirds of the isomer are in the *Z*- conformation implying a sufficiently high stability of the *Z*-form even at temperatures of 50 °C. A possible determination of the LCST is the measurement of the light transmission at 700 nm as the precipitation of the polymer at the LCST increases the sample turbidity leading to a decreasing light transmission. The results for the determined LCST can be found in Table S1.

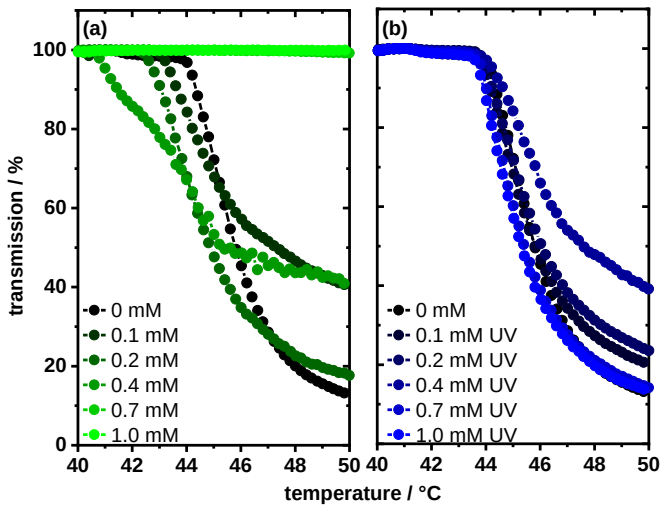

Figure S2. Light ttransmission at 700 nm of 0.5 g/L HPC with different surfactant concentrations under (a) green light and (b) UV light with a heating rate of 0.1 K/min.

2.2 Dynamic Light Scattering (DLS).

Figure S3 shows the hydrodynamic radius as a function of temperature as well as for different light irradiation that resulted in different predominant conformation (E vs Z) of the AAP surfactant. Further information and a detailed discussion is provided in the main text.

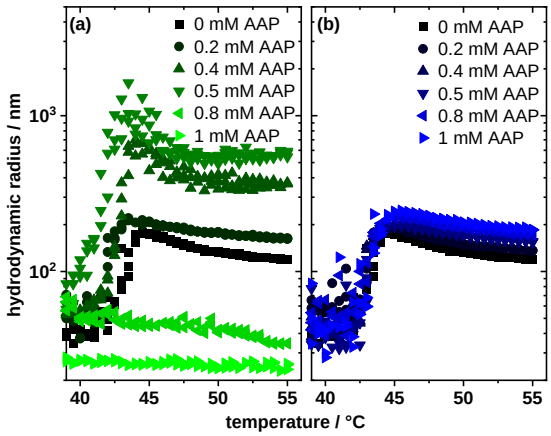

Figure S3. Hydrodynamic radius of a filtered (0.2 µm) 0.05 g/L HPC solution for different surfactant concentrations and for (a) green light and (b) UV light irradiation as a function of temperature. The temperature was changed for the experiments using a heating rate of 3.3 K/h.

Besides the hydrodynamic radius the backscattered light can be determined by the DLS measurement. The beforementioned turbidity at the LCST leads to a sharp increase of the intensity of the backscattering light (see Figure S4). This implies that the count rate from the DLS experiments can be used complementary to the measurement of the light transmission at 700 nm as both methods are based on the changes of the samples' light scattering.

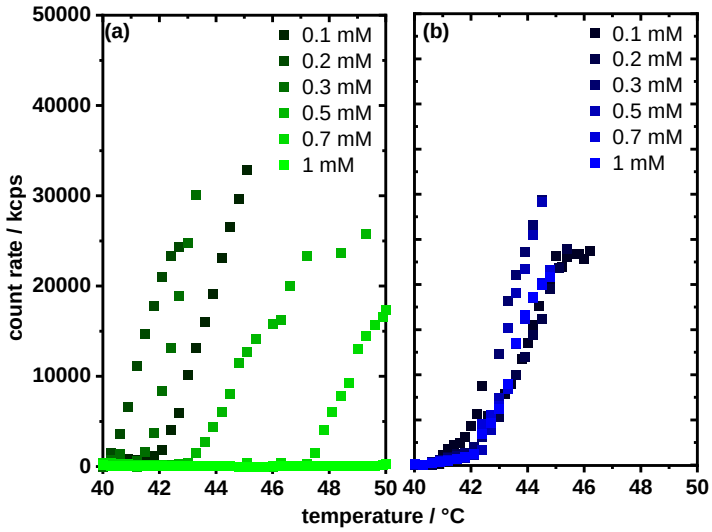

Figure S4. Count rate from the DLS experiments of mixtures consisting of 0.5 g/L HPC and different surfactant concentrations under (a) green light and (b) UV light irradiation while the temperature was changed at a rate of 3.3 K/h.

2.3 Shear rheology.

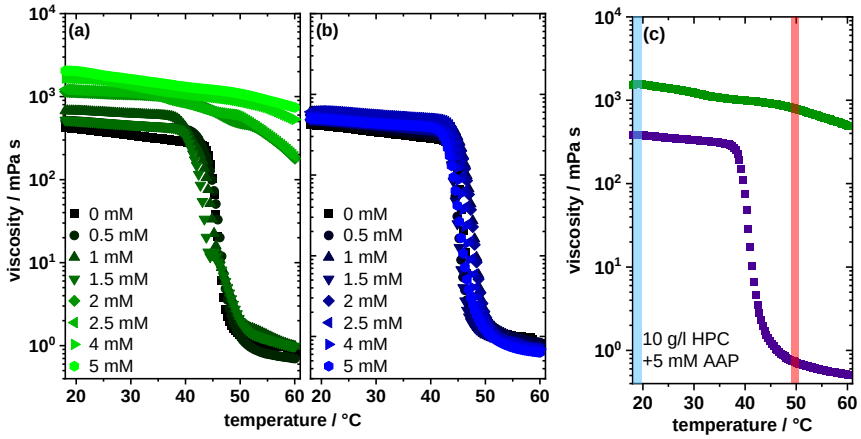

Figure S5. Temperature dependent viscosity of mixtures with 10 g/L HPC and variable AAP surfactant concentration at a shear rate of 50 s^{-1} and a heating rate of 0.45 K/min under (a) green irradiation and (b) UV irradiation. (c) Highlights the obtained viscosity curve with 5mM AAP under green or UV irradiation as with vertical marks the temperatures used for the dynamic viscosity experiments in the main text are indicated.

Figure S6 we show a demonstrator experiments that highlight the dramatic changes in sample viscosity and which are complementary to what is presented in the main text in Figures 2 and 4. For the results in Figure S6, the sample tube was placed in a 50 °C hot bath and a stirring fish was dropped into the tube at time zero. Clearly drastic changes in velocity of the stirring fish inside the solution with a HPC/AAP occur as a function of light irradiation and are linked to the changes in the samples viscosity by several orders of magnitude (see Figure S5 and main text for discussion).

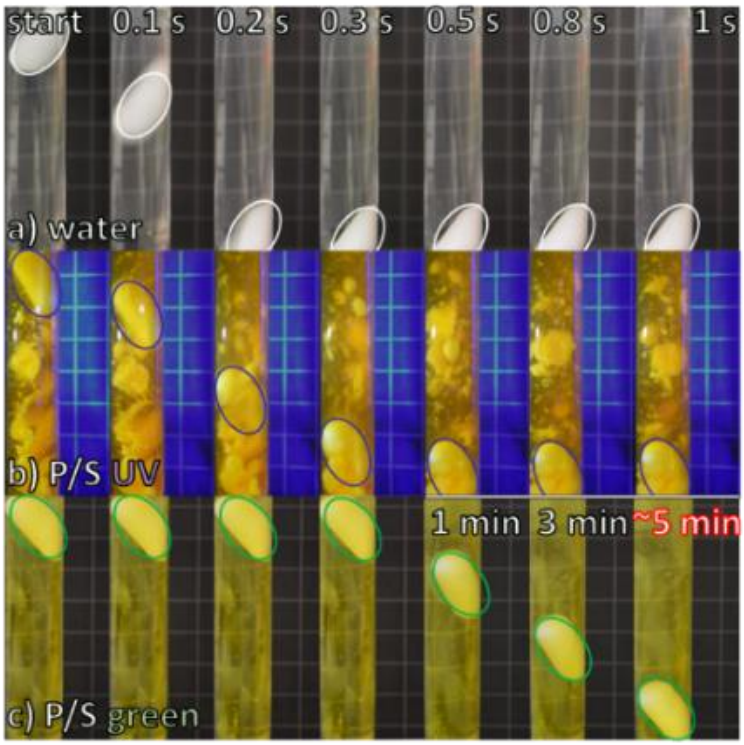

Figure S6. Demonstration experiment of the viscosity change of a mixture consisting 10 g/L HPC and 5 mM AAP in a 50 °C hot bath under (b) UV and (c) green irradiation by observing the falling velocity of an object in the respective media. A water sample (a) is shown as a reference.

2.4 ^{1}H HR-MAS NMR.

At thermal equilibrium both AAP isomers, *E*-AAP and *Z*-AAP, are present as recently discussed by Honnigfort et al.[1] However, after irradiation with UV light (365 nm) only the AAP *Z*-isomer is present (cf. Figure S7). The spectral differences between *E*-AAP and *Z*-AAP can also be observed in the 2D ^{1}H-^{1}H RFDR NMR spectra recorded under HR-MAS conditions in Figure S8. Here, the 2D NMR spectrum of the E-isomer includes all expected ^{1}H-^{1}H correlations for both the *E*- and *Z*-isomers (cf. Figure S8a,b). Note that the intensity of the *Z*-isomer is much lower (~10 %) compared to the *E*-isomer in agreement with our previous results.[1] In the ^{1}H HR-MAS NMR spectrum of HPC (Figure S7b) two proton signal regions are present. The methyl group of the side chain at 1.1 ppm (grey) and the overlapping ^{1}H signals between 3 and 4 ppm (orange) arise from the side chain (R) and the HPC polymer backbone and cannot be further distinguished. The ^{1}H chemical shift of the pure and dissolved *E*-/*Z*-AAP surfactants in FigureS7a a change slightly (~ ±0.1 ppm) in the mixture with HPC (Figure 3). Figure S7c shows the mixture of 5 g/L HPC with 5 mM AAP recorded at different MAS rates, demonstrating that a MAS frequency of 2.0 kHz is sufficient to remove sample susceptibility effects and reduce the ^{1}H-^{1}H dipolar broadening caused by the aggregated state and slow molecular tumbling of the AAP-HPC system in solution. However, the spinning side bands from the intense water signal, marked by asterisks, are overlapping with the ^{1}H signals of interest at this MAS rate. Thus, employing a MAS rate of 5.0 kHz moves the first spinning side bands outside the ^{1}H chemical shift range at the employed magnetic field of 11.76 T (500.39 MHz). The elucidation of the interaction between the AAP surfactants and HPC were recorded under these HR-MAS conditions using 2D ^{1}H-^{1}H RFDR NMR experiments as described in the main text (Figure 3).

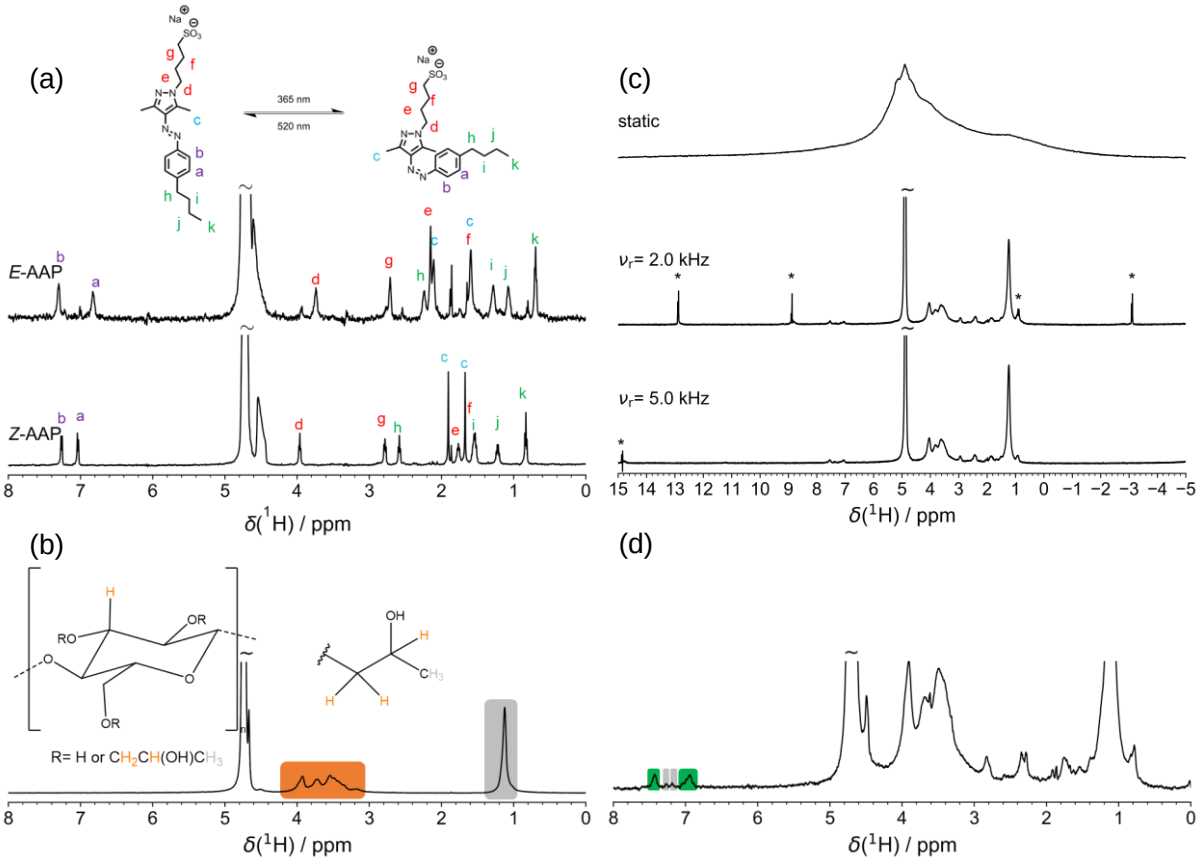

Figure S7. ^{1}H HR-MAS NMR spectra of (a) 5 mM *E*- and *Z*-AAP and (b) 5 g/L HPC in D_2O recorded at 11.76 T employing a MAS frequency of 5.0 kHz. The signal assignment for *E*-/*Z*-AAP is done by small letters and color coded HPC. The signals of the minor *Z*-AAP component in *E*-AAP are marked by an asterisk. (c) Mixture of 5 g/L HPC + 5 mM AAP recorded without MAS (static) and at different MAS rates. Spinning side bands are marked asterisks. (d) ^{1}H-HR MAS spectrum of 5 mM E-AAP with 10 g/L HPC that was recorded at 5.0 kHz MAS. The integration regions to determine the photostationary state of E / Z AAP (85:15 ± 7 %) are shown in green and grey, respectively.

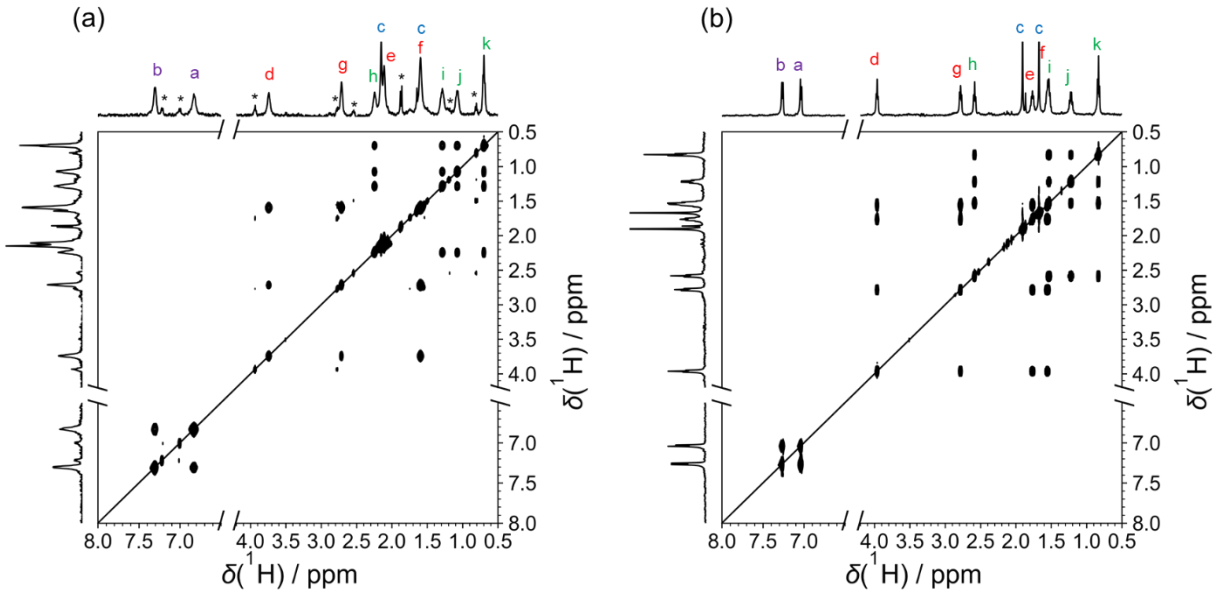

Figure S8. 2D ^{1}H-^{1}H RFDR NMR spectra of 5 mM (a) *E*-AAP and (b) *Z*-AAP in D_2O recorded at 11.76 T and 302 K under HR-MAS conditions employing a MAS frequency of 5.0 kHz. A RFDR dipolar recoupling time of 64 rotor periods (102.4 ms) was used in both spectra.

The critical transition temperature (T_c) of the coil-to-globule transition of HPC have also been investigated using variable-temperature ^{1}H HR-MAS experiments. Due to the stronger aggregation with increasing temperature for HPC, the effective T_2 relaxation time for ^{1}H is decreasing and is eventually reduced below the spectrometer dead time. This results in a characteristic loss of intensity for the ^{1}H signals of HPC. Figure S9 shows the variable-temperature ^{1}H HR-MAS spectra of HPC recorded from 302 to 342 K. The ^{1}H signal intensity of the HPC backbone (3.0 to 4.0 ppm) and the signal of the side-chain methyl group (1.1 ppm) are both clearly decreasing with increasing temperature. The signal of the HDO peak is shifting due to its well-known temperature-dependent ^{1}H chemical shift.

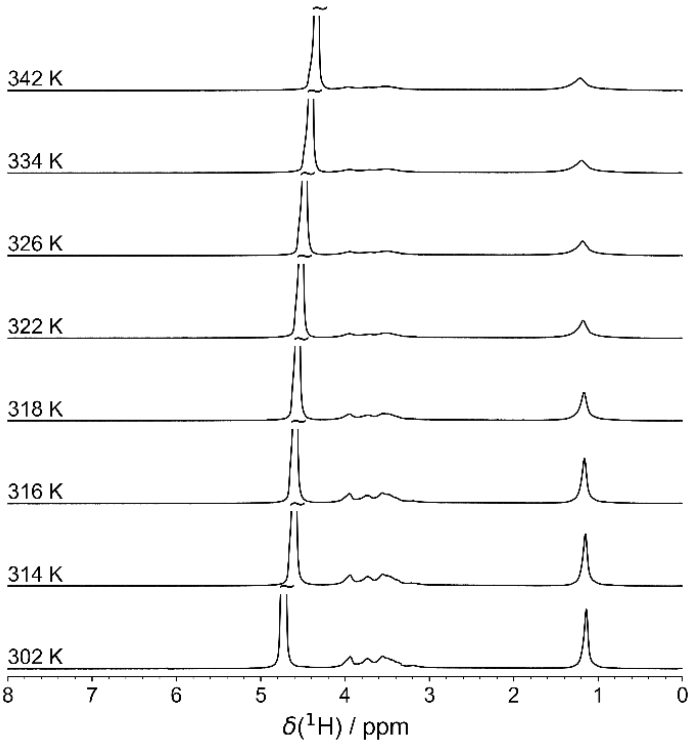

Figure S9. Variable-temperature ^{1}H HR-MAS NMR spectra of HPC (5 g/L in D_2O) recorded at 11.76 T (500.39 MHz) employing a MAS frequency of 5.0 kHz.

The loss of signal intensity with increasing temperature can be fitted using the following equation.[9]

$$\frac{I}{I_{MAX}} = \frac{a}{1+e^{(-k\cdot(T_c-T))}} + b \qquad \text{(S1)}$$

Here, T_c is the critical transition temperature and *a* and *b* are fit parameters. To obtain a valid transition temperature an upper and lower plateau value have to be reached. Since the upper temperature is limited by the boiling point of D_2O, no second plateau was reached for the higher concentrations of E-AAP (5 and 10 mM). However, a value could be estimated by the fitting procedure. Figure S10 summarizes the temperature-dependent values of I / I_{max} for the HPC backbone (Figure S10a,c) and the methyl group of the side-chain R (Figure S10b,d) for the E- (Figure S10a,b) and Z-isomer (Figure S10c,d), respectively. The optimized values from the fitting procedure are summarized in Table S1.

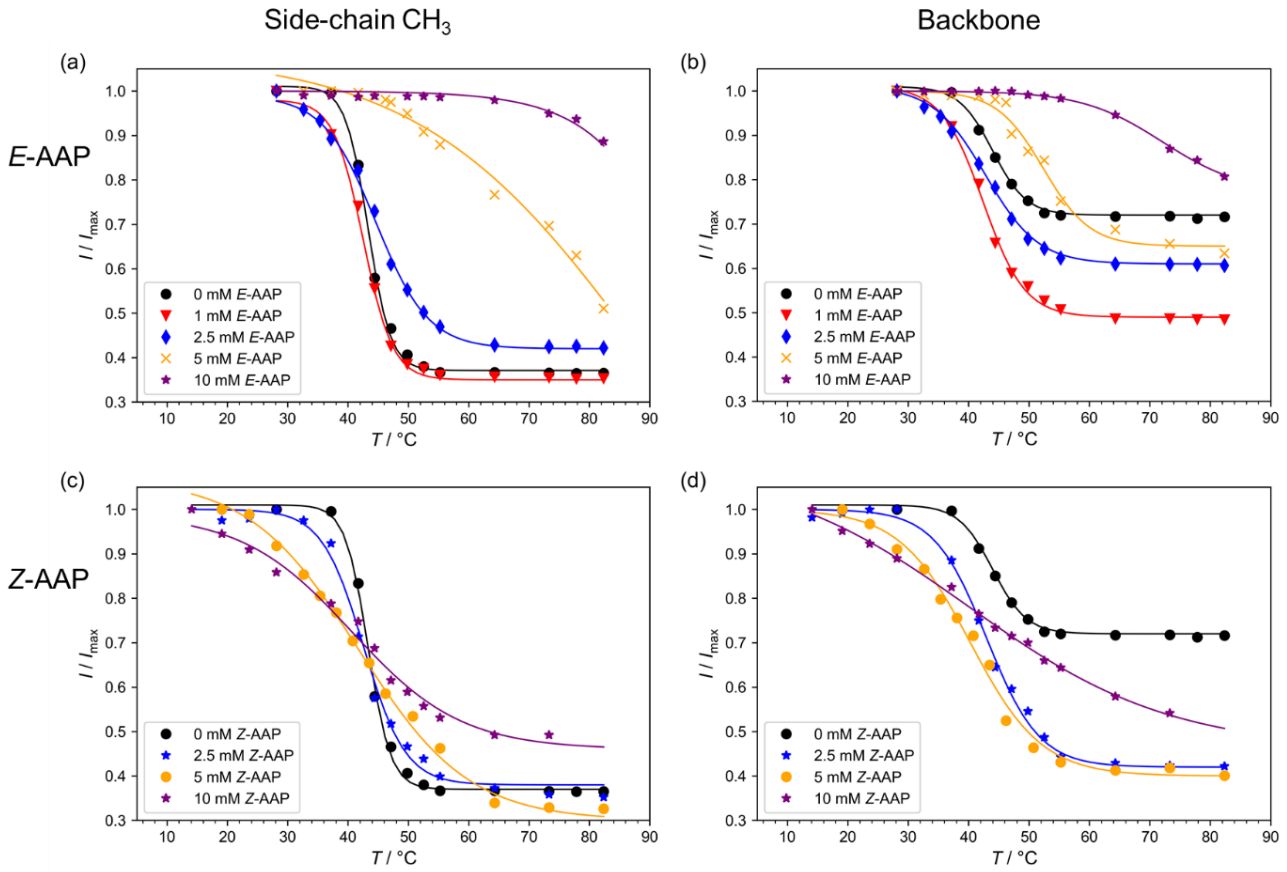

Figure S10. Normalized intensity decay for different concentrations of (a, b) *E*-AAP and (c, d) *Z*-AAP in 10 g/L HPC following the ^{1}H signals at (a, c) 3.0-4.0 ppm and (b, d) 1.1 ppm, respectively, as marked in Figure S6. The solid lines correspond to the optimized values in Table S1 using Eq. S1.

2.5 Differential Scanning Calorimetry (DSC).

Figure S11a shows the DSC traces of HPC solutions with varying AAP content after green or UV irradiation, respectively. In all cases a small, but clearly detectable endothermic peak was observed. The intersection of the dashed line on each trace indicates the onset temperature. The deviation of the onset temperature from surfactant-free solutions is given in Figure S11b.

While after blue irradiation no effect of Z-AAP on the phase transition of HPC is observed, the E form after green irradiation causes distinct changes: At low concentrations of E-AAP T_c is shifted to slightly lower values, while at higher concentrations c > 0.2 mM the transition is shifted to higher temperature.

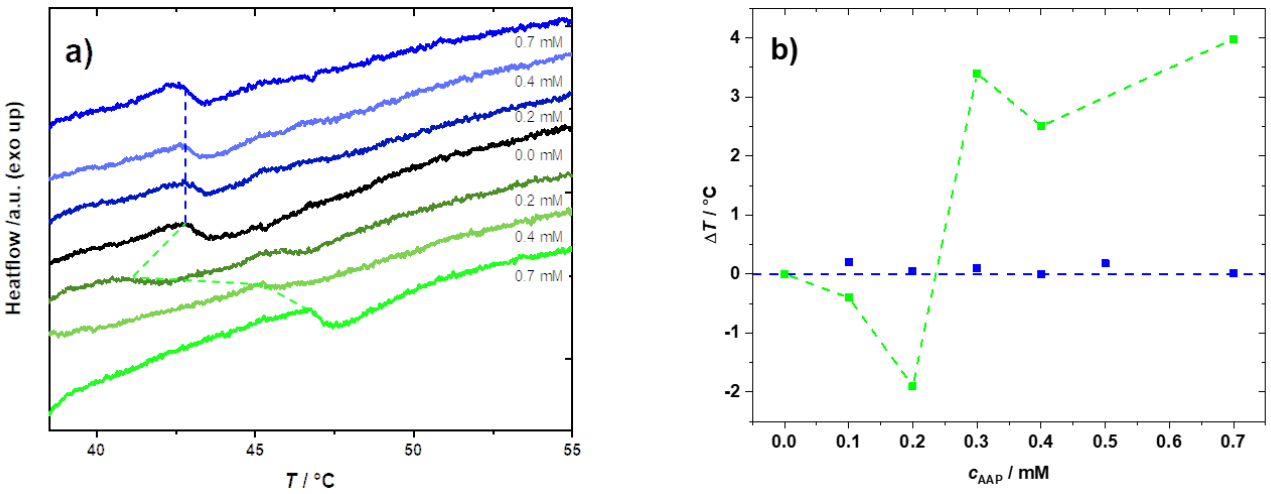

Figure S11. a) Heat flow traces of solutions with 0.5 g/L HPC and varying concentrations of AAP and b) Shift of the onset temperature with respect to surfactant-free HPC solution. Irradiation prior to measurement was performed with UV light (blue traces and data points) or visible light (green traces and data points).

References

[1] C. Honnigfort, R. A. Campbell, J. Droste, P. Gutfreund, M. R. Hansen, B. J. Ravoo, B. Braunschweig, *Chem. Sci.* **2020**, *11*, 2085.
[2] J. Stetefeld, S. A. McKenna, T. R. Patel, *Biophys. Rev.* **2016**, *8*, 409.
[3] R. Pecora, *Journal of Nanoparticle Research* **2000**, *2*, 123.
[4] T. G. Mezger, *Das Rheologie Handbuch. Für Anwender von Rotations- und Oszillations-Rheometern*, Vincentz Network, Hannover, **2016**.
[5] A. E. Bennett, R. G. Griffin, J. H. Ok, S. Vega, *J. Chem. Phys.* **1992**, *96*, 8624.
[6] A. Ramamoorthy, J. Xu, *J. Phys. Chem. B* **2013**, *117*, 6693.
[7] H. E. Gottlieb, V. Kotlyar, A. Nudelman, *The Journal of organic chemistry* **1997**, *62*, 7512.
[8] D. S. Raiford, C. L. Fisk, E. D. Becker, *Analytical Chemistry* **1979**, *51*, 2050.
[9] A. Larsson, D. Kuckling, M. Schönhoff, *Colloids and Surfaces A: Physicochemical and Engineering Aspects* **2001**, *190*, 185.